JOURNAL OF MATERIALS SCIENCE 31 (1996) 1915–1923

Viscoelastic behaviour of symmetrical three layer beams

P. CUILLERY, L. DAVID, S. ETIENNE
Institut National des Sciences Appliquées, Groupe d'Etudes de Métallurgie Physique et de Physique des Matériaux 69621, Villeurbanne cedex, France

M. MANTEL
Ugine S.A., Centre de Recherches d'Ugine, 73403 Ugine, France

Using the theory of linear elasticity, a solution to the torsion problem of the symmetrical three-layer beam is proposed. In this way, the complex torsional stiffness has been determined. The predicted values are then compared with experimental results obtained by mechanical spectroscopy operated in the torsion mode. The shifts in temperature, observed between the loss factor maximum exhibited by the polymers and the sandwiches, respectively, are mainly attributed to a mechanical coupling effect instead of an interphase effect.

1. Introduction

Symmetrical sandwich steel/polymer/steel sheets have been developed to reduce noise and vibrations in structures. Thanks to the main relaxation phenomenon associated with the glass transition of polymer materials, high loss factors together with significant stiffnesses are expected. Mechanical spectroscopy operated in sinusoidal torsional stress is used to characterize the damping factor. The study compares mechanical relaxations exhibited on one hand, by the sandwich and on the other hand, by the polymeric part alone. Experiments show that the shape of the loss factor peak is affected and its maximum is shifted in temperature from the polymer to the sandwich.

In order to estimate the interface or interphase effects on this temperature shift and more generally the polymer microstructure influence, it is necessary to study first the mechanical coupling in the sandwich assuming perfect interfaces. The aim of this work is to predict the sandwich behaviour from the characteristics of its components measured separately. A theoretical determination of the symmetrical sandwich complex stiffness has been developed. This calculation is based on the resolution of the elastic torsion problem. Then theoretical and experimental results are compared and discussed.

2. Theoretical determination of viscoelastic characteristics of symmetrical sandwiches

2.1. The elastic torsion problem

The problem of the torsion of beams consisting of isotropic materials is presented below.

2.1.1. General equations

Let the coordinate system be as depicted on Fig. 1. Oz is the twisting axis while Ox and Oy define the cross-sections. All materials of the bar are assumed homogeneous and isotropic. Basically, the cross-section S of the bar consists of several regions S_0, S_1, S_2, ... , S_m corresponding to different materials.

The boundary conditions of the torsion problem are considered, assuming, as for the case of a homogeneous bar, that cross-sections twist and warp. This supposition leads to the expressions for the displacement components:

$$u = -\gamma zy, \quad v = \gamma zx, \quad w = \gamma\varphi(x, y)$$

where γ is the relative twist (i.e. the angle of the torsion per unit length) and φ the torsion function used to define the warping.

Hooke's law relate the stress components in each region S_i corresponding to the displacements:

$$\sigma_{xz} = \mu_i\gamma\left(\frac{\partial\varphi_i}{\partial x} - y\right), \quad \sigma_{yz} = \mu_i\gamma\left(\frac{\partial\varphi_i}{\partial y} + x\right)$$

where μ_i and φ_i are the shear modulus and the torsion function, respectively, in the region S_i.

Far below the resonance frequencies, it is easily seen that the substitution of these expressions in equilibrium equations leads to the Laplace equation, as in the case of homogeneous bars:

$$\Delta\varphi = 0$$

Thus, in the present case, the function φ must also be harmonic in each region S_i. The difference from the case of the homogeneous bar manifests only in the boundary conditions. These conditions express that:

(i) the external surface of the beam is free from external forces,

0022–2461

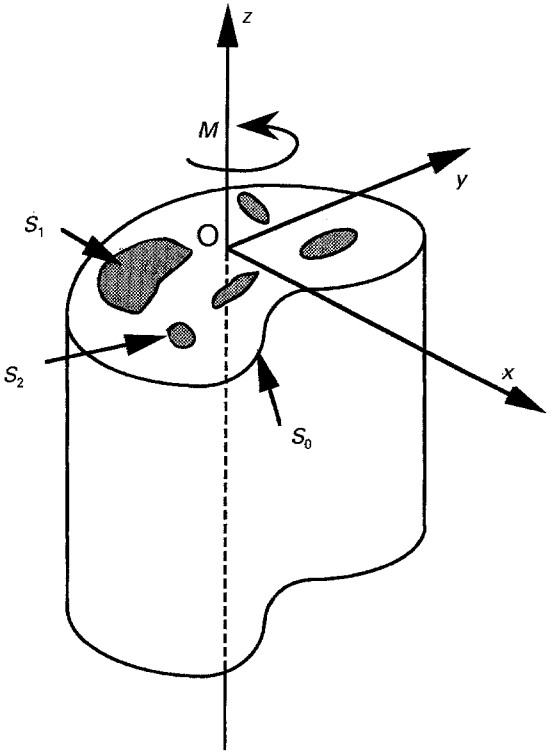

Figure 1 Torsion of a compound beam. The cross-section is a set of $S_1 \ldots S_n$ regions of different materials in the surrounding region S_0.

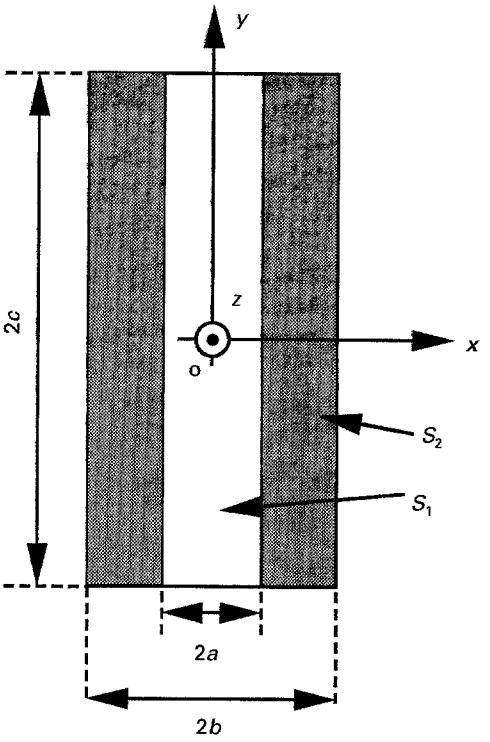

Figure 2 Torsion of a sandwich. The cross-section is a set of S_1 and S_2 regions of the materials 1 and 2. Oy is a symmetry axis in the cross-section.

(ii) the forces acting on the elements of the surface separating the different materials are equal in magnitude and opposite in direction,

(iii) the displacements u, v, w remain continuous across the interfaces, which are assumed to be perfect.

The force moment M is obtained by calculating the moment resulting from all the forces with respect to the Oz axis:

$$M = \int_S (-y\sigma_{xz} + x\sigma_{yz})\,dS$$

resulting in:

$$M = \sum_i \int_{S_i} \gamma\mu_i \left(x^2 + y^2 + x\frac{\partial\varphi_i}{\partial y} - y\frac{\partial\varphi_i}{\partial x}\right) dx\,dy$$

2.1.2. Torsion of a sandwich

Consider the symmetrical sandwich (Fig. 2). Its external dimensions are equal to $2b$ and $2c$ and the width of the central material section is equal to $2a$. S_1 and S_2 are the regions occupied by the two materials. Let their shear moduli be μ_1 and μ_2, respectively. The Oz axis is the twist axis as quoted above and Ox, Oy axes are chosen with respect to the cross-section symmetries. The functions φ_1 and φ_2 represent the torsion function φ in S_1 and S_2 regions, respectively.

In order to solve this problem, it is convenient to split the cross-section along the symmetry axis Oy. The result thus obtained on the two-layer material is simply half of the sandwich stiffness. A torsion function form developed for the torsion of two-layer beams [1] can be used. A solution procedure for the functions φ_1 and φ_2 and then from these the complex rigidity is presented in the appendix.

2.2. Viscoelastic characteristics of a sandwich

The shear moduli introduced in the solution presented above are implicitly real quantities.

Assuming the correspondence principle [2], the complex stiffness of a mechanical system can be deduced from the calculation of the stiffness supposing first each component elastic, and then replacing each modulus with its complex expression. The viscoelastic properties thus calculated are usually represented by the real part of the complex stiffness and the loss factor, i.e. the ratio of imaginary part to real component of this stiffness.

From the expression presented in the appendix, a computer program has been developed, thus allowing numerical simulations of the complex rigidity as a function of temperature and geometrical parameters for the sandwich structure.

3. Experimental and theoretical results

3.1. Materials and methods

The stainless steel foils used were supplied by UGINE S.A., France. The thickness was 200 μm and the surface state (bright anneal) was obtained by annealing the stainless steel at 850 °C in a non-oxidizing N_2/H_2 atmosphere. Before processing, the foils were cleaned with acetone and cut into 300×300 mm^2 pieces.

Two different polymers were considered in this work.

The first polymer used was an ethylene-vinyl acetate copolymer (EVA). It was a 100 μm thick film which was placed between two stainless steel foils and the sandwich was pressed with heater platens under a pressure of 0.1 MPa at 200 °C for 10 min.

A polyacrylic (PAc) was used as the second polymer. It is a 110 μm thick film which was used as an adhesive.

The specimens suitable for mechanical spectroscopy testing were cut from 300×300 mm^2 sandwich pieces, and the dimensions were about 70×7 mm^2.

Dynamic mechanical spectroscopy was performed in torsion by means of two home made instruments. A high resolution set-up [3] was used to investigate unsupported polymeric thin films. Sandwiches and steel foils were characterized by a more classical spectrometer [4].

3.2. Preliminary remark

The quantity that is measured through mechanical spectroscopy is the overall torsional stiffness of the specimen. In the case of isotropic and homogeneous bars, this stiffness is the product of the shear modulus and a quantity F_S called the shape factor, which only depends on sample dimensions and geometry. For the symmetrical sandwiches used (Fig. 2), $F_S = \frac{16}{3} cb^3$.

In the scope of this work, composite structures are considered. It is then convenient to define the apparent shear modulus as the shear modulus of an homogeneous and isotropic equivalent sample that would present the same stiffness and the same external dimensions as the sample under test.

3.3. Experimental results

The measurements have been carried out for separate materials and composites, namely:

—stainless steel foils (Fig. 3)

—EVA and a stainless steel/EVA/stainless steel foils sandwich (Figs 4 and 5), thus enabling the prediction of the metal/polymer/metal configuration behaviour.

—PAc film and a PAc/stainless steel foils/PAc sandwich (Figs 6 and 7), in order to study polymer/metal/polymer configuration.

The viscoelastic characteristics of the metallic foils are shown in Fig. 3. The loss factor (which is defined as $G''/G' = \tan\Phi$) remains nearly constant and equal to 2×10^{-3}. The shear modulus is equal to 59 GPa at 295 K and its temperature coefficient is about -0.025 GPa K^{-1}.

The viscoelastic characteristics of the polymers are depicted on Figs 4 and 6 and are to be compared to the corresponding characteristics of the sandwiches (Figs 5 and 7).

Obviously, from the polymer to the sandwich, the loss factor decreases, and the real part of the sandwich apparent modulus is lower than the real part of the stainless steel modulus, as expected. Less obvious are the shifts observed between the mechanical relaxations of polymers and mechanical relaxations of sandwiches. For the stainless steel/EVA/stainless steel foils, the shift is $+10$ K, and for the other configuration (PAc/stainless steel/PAc) the shift reaches -32 K.

The experimental results of Fig. 3 (stainless steel) and Fig. 4 (EVA polymer) are computed according to the mechanical coupling model previously determined, and can be compared with the data directly obtained with the corresponding metal/polymer/metal sandwich. This comparison is shown in Figs 8 and 9 for the loss factor and the real part of the

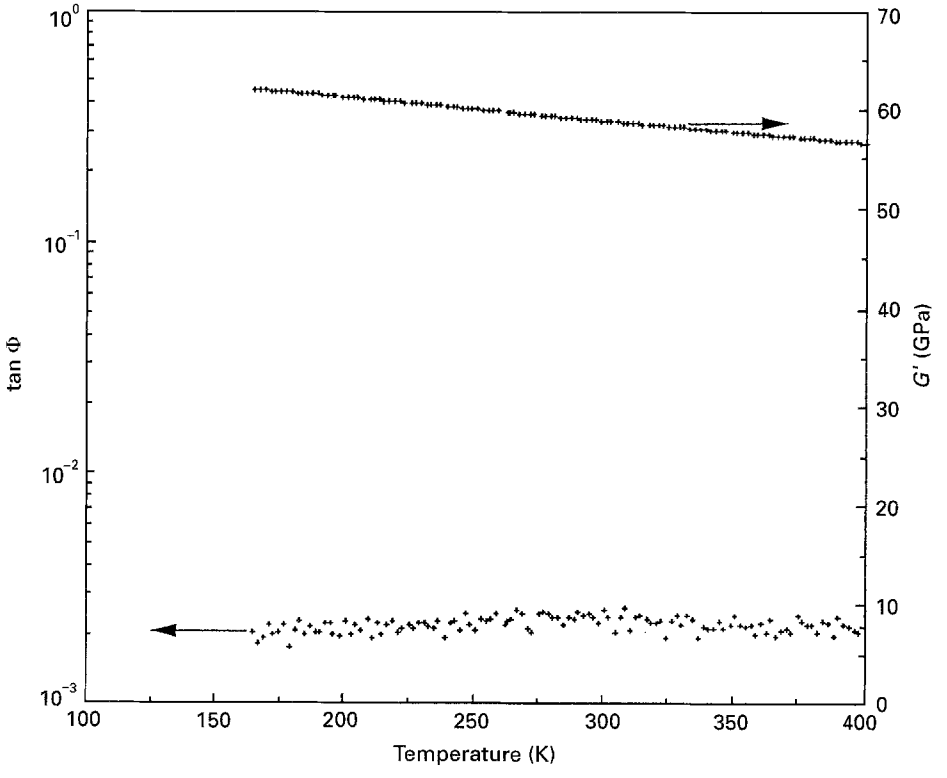

Figure 3 Isochronal (at a fixed frequency, $f = 1$ Hz) variation of the loss factor $\tan\Phi$ and the real part of the shear modulus G' of the stainless steel foils against temperature.

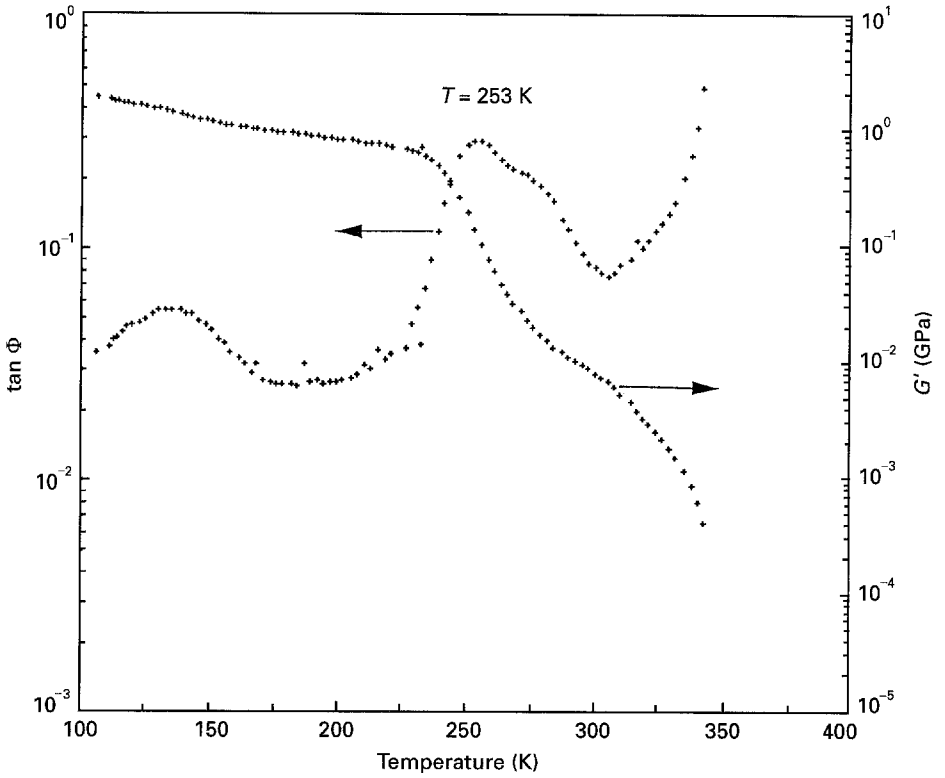

Figure 4 Isochronal (at a fixed frequency, $f = 1$ Hz) variation of the loss factor tan Φ and the real part of shear modulus G' of EVA polymer film with temperature. The maximum of the tan Φ value, associated with the glass transition mechanical relaxation, occurs at $T = 253$ K.

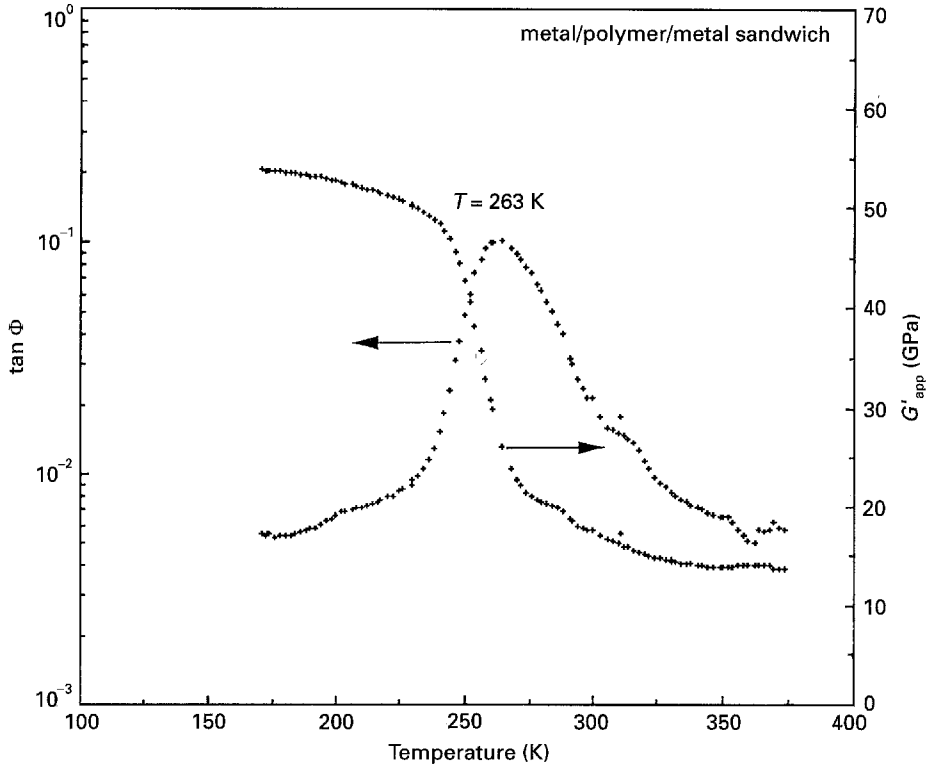

Figure 5 Isochronal (at a fixed frequency, $f = 1$ Hz) variation of the loss factor tan Φ and the real part of apparent shear modulus G'_{app} of stainless steel/EVA/stainless steel sandwich with temperature. The maximum of the tan Φ value occurs at $T = 263$ K.

apparent shear modulus, respectively. The polymer/metal/polymer configuration is also studied according to the same frame of analysis, but for PAc and PAc/stainless steel/PAc structure. The comparison between experimental and calculated data are displayed in Figs 10 and 11 for the loss factor and the real part of the apparent shear modulus, respectively.

It is easily seen that the law predicts the shear modulus and the loss factor of sandwiches from their components characteristics for the two different

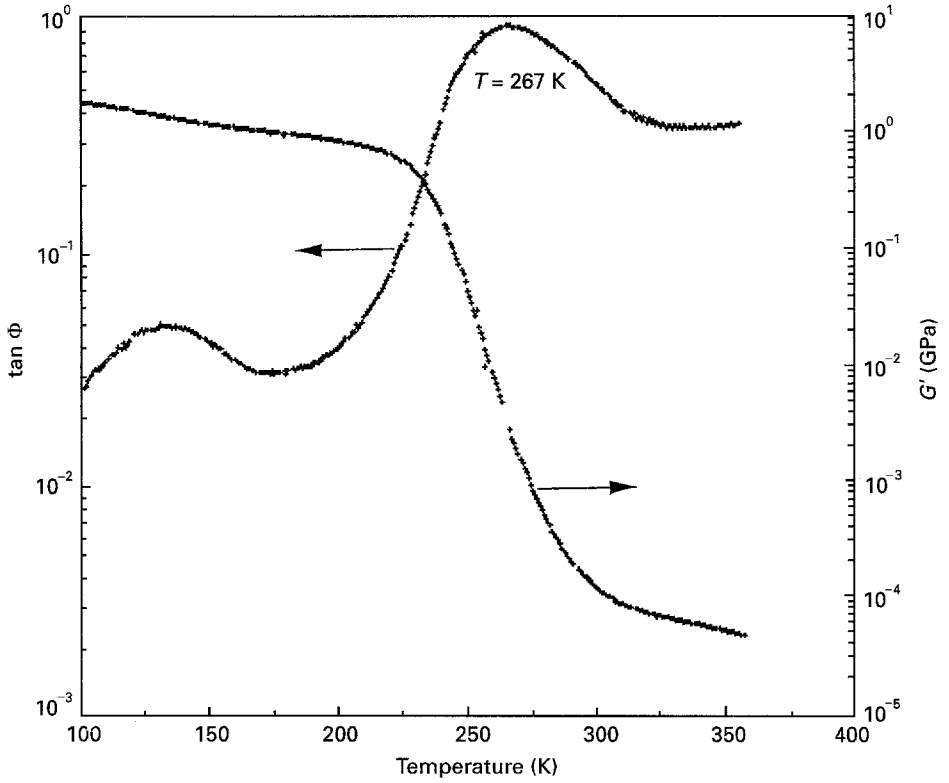

Figure 6 Isochronal (at a fixed frequency, $f = 1$ Hz) variation of the loss factor $\tan\Phi$ and the real part of shear modulus G' of PAc polymer film with temperature. The maximum of the $\tan\Phi$ value, associated with the glass transition mechanical relaxation occurs, at $T = 267$ K.

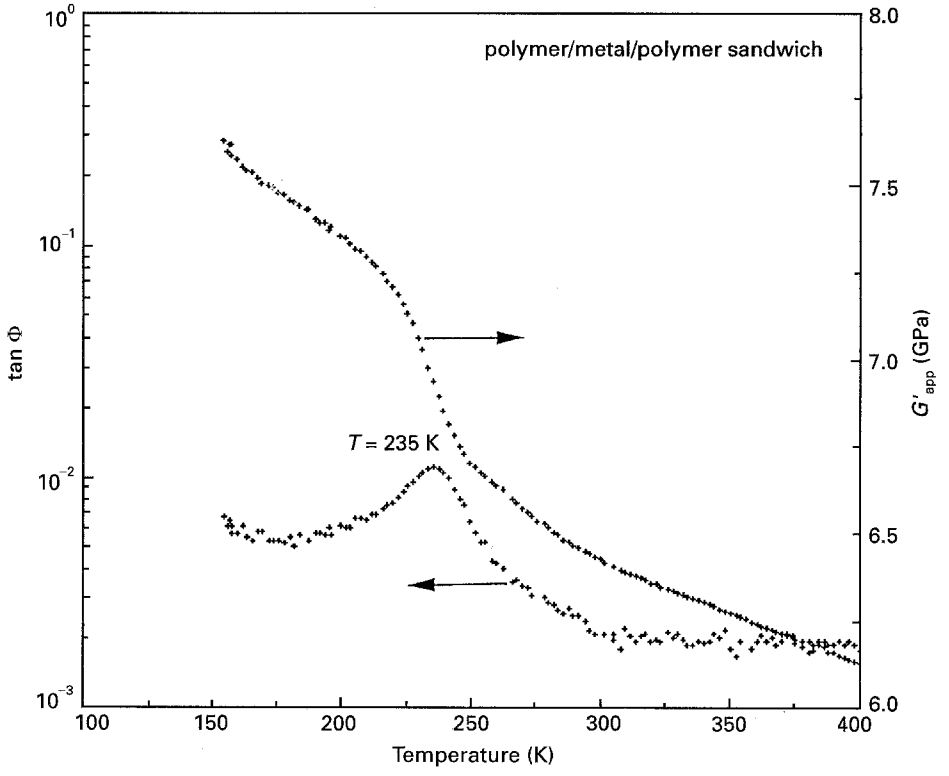

Figure 7 Isochronal (at a fixed frequency, $f = 1$ Hz) variation of the loss factor $\tan\Phi$ and the real part of apparent shear modulus G'_{app} of PAc/stainless steel/PAc sandwich with temperature. The maximum of the $\tan\Phi$ value occurs at $T = 235$ K.

configurations made of the two different polymers under consideration. Specially, the shift of $\tan\Phi$ maxima are well reproduced. The comparison should probably be improved if modulus were measured with an accuracy better than 15%. Nevertheless the experimental determination of shear modulus variations, as well as the loss factor, are more accurate (3%).

The limitation of the comparison of experimental and calculated data arises first from the violation of

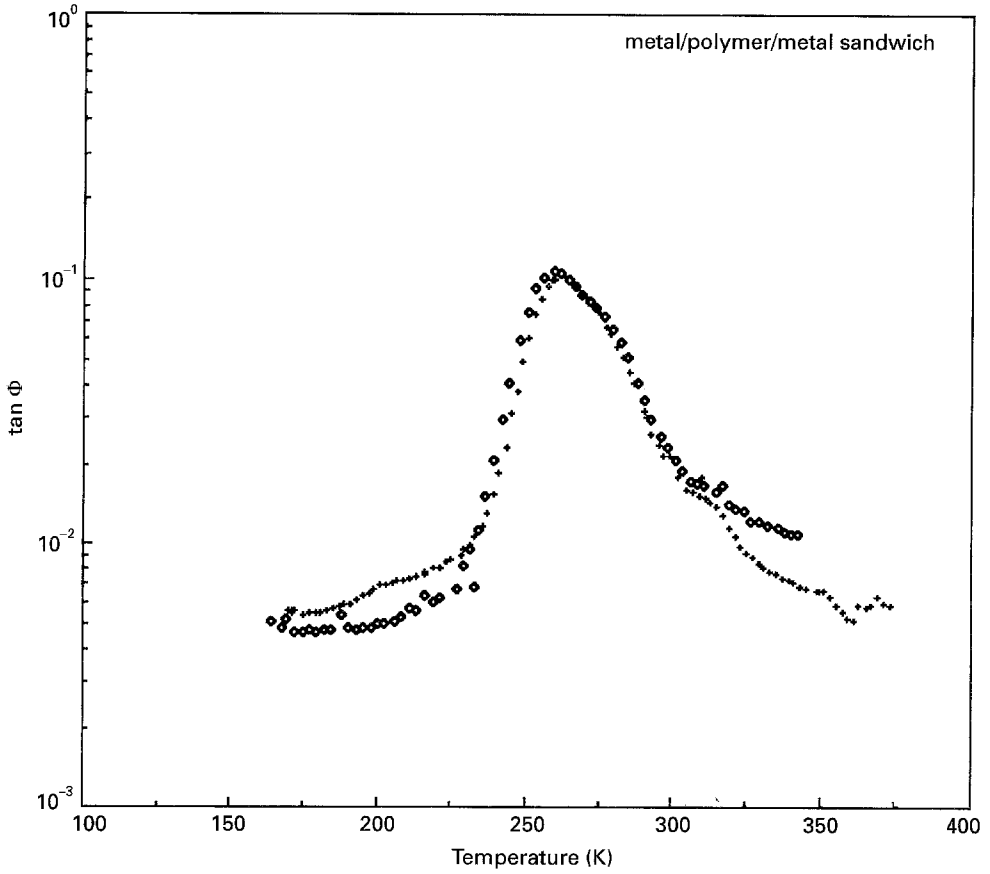

Figure 8 Comparison of experimental loss factor results for (i) stainless steel/EVA/stainless steel sandwich and (ii) calculated values, resulting from the mechanical coupling model and experimental behaviours of the stainless steel and the EVA polymer (Figs 3 and 4, respectively). Key: + experimental data, ◇ calculations.

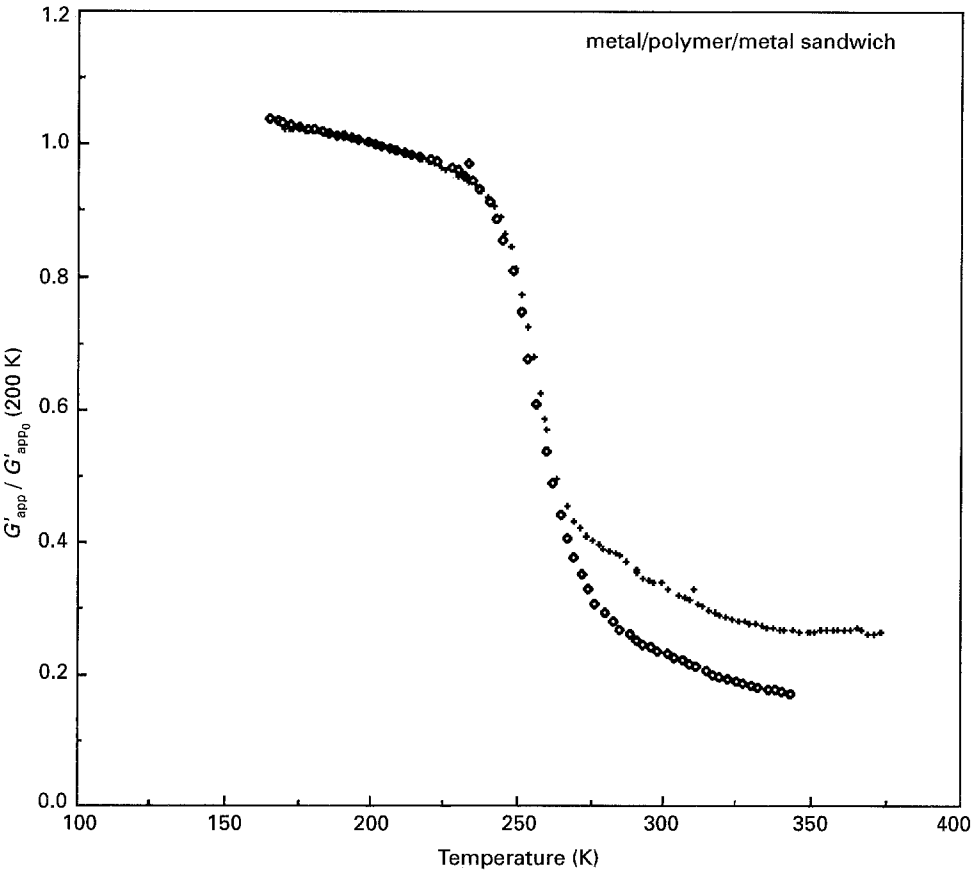

Figure 9 Comparison of experimental real apparent shear modulus results for (i) stainless steel/EVA/stainless steel sandwich and (ii) calculated values, resulting from the mechanical coupling model and experimental behaviours of the stainless steel and the EVA polymer (Figs 3 and 4, respectively). G'_{app_0} is the real apparent shear modulus value measured or predicted at $T = 200$ K ($G'_{app_0} = 52.7$ GPa and the calculation leads to $G'_{app_0} = 48.7$ GPa). Key: + experimental data, ◇ calculations.

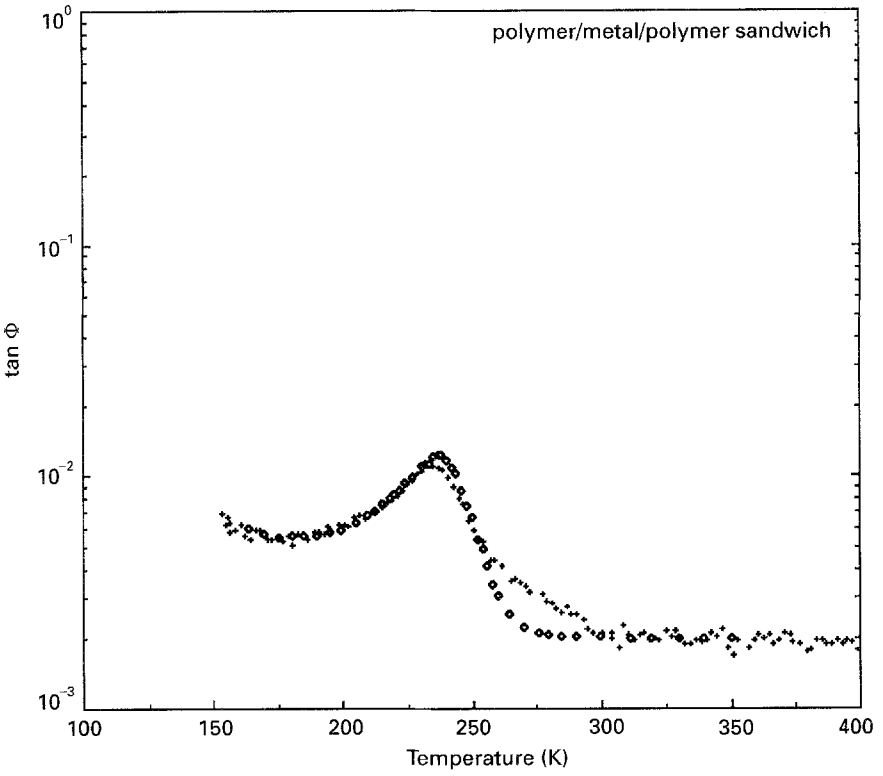

Figure 10 Comparison of experimental loss factor results for (i) PAc/stainless steel/PAc sandwich and (ii) calculated values, resulting from the mechanical coupling model and experimental behaviours of the stainless steel and the PAc polymer (Figs 3 and 6, respectively). Key: + experimental data, ◇ calculations.

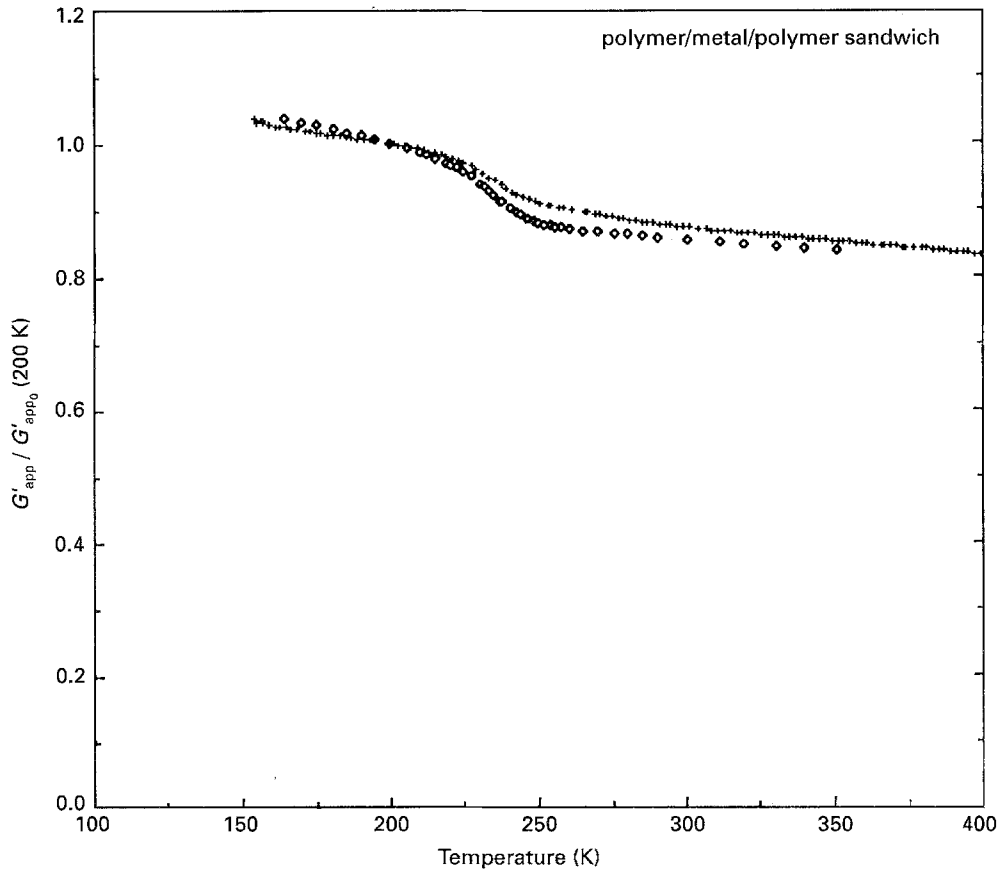

Figure 11 Comparison of experimental real apparent shear modulus results for (i) PAc/stainless steel/PAc sandwich and (ii) calculated values, resulting from the mechanical coupling model and experimental behaviours of the stainless steel and the PAc polymer (Figs 3 and 6, respectively). G'_{app_0} is the real apparent shear modulus value measured or predicted at $T = 200$ K ($G'_{app_0} = 7.36$ GPa and the calculation leads to $G'_{app_0} = 6.85$ GPa). Key: + experimental data, ◇ calculations.

the St-Venant principle near the jaws. In the polymer/metal/polymer configuration, we noticed that the creep of the polymer near the jaws induces a large departure from the calculated value. Thus, it is worthwhile to notice that in the case of the PAc/stainless steel/PAc sandwich actually tested, the polymer material covers only the useful part of the sandwich (there is no polymer in the jaws). In the case of metal/polymer/metal structure, this creep effect could be responsible for the difference observed above 300 K between calculated and experimental results in Figs 8 and 9.

The second limitation of the comparison, results from the non-exact superimposition of the twist axis and the sample symmetry axis, although it is assumed that both are equivalent in the theoretical section.

In the literature, interpretations of change of loss modulus peak or shear modulus of sandwich structures in terms of interphases or surface dislocations effects are often found [5, 6]. The coupling analysis, as it is shown here (in the case of the torsion stress applied to sandwiches), is actually essential to understand the mechanical relaxations of sandwiches linked to polymer mechanical relaxations.

4. Conclusion

The viscoelastic behaviour of symmetrical three-layer beams has been analysed. The calculated values fall in good agreement with the experimental data assuming perfect interfaces between components.

The major conclusion is that, at least for the specimens studied here, the shifts observed between the mechanical relaxations of the unsupported polymers and the sandwiches are mainly attributed to a mechanical coupling effect, instead of an interphase effect, as often claimed in the literature.

Acknowledgements

The authors are grateful to UGINE SAVOIE for financial support, and to Professor J. Perez for helpful discussions.

Appendix

The harmonic functions φ_1 and φ_2 will be determined in the following forms:

$$\varphi_1(x, y) = \vartheta_1(x, y) - xy$$

$$\varphi_2(x, y) = \vartheta_2(x, y) - xy$$

where:

$$\vartheta_1(x, y) = \sum_{n=0}^{+\infty} A^1_{2n+1} \sinh mx \sin my$$

$$\vartheta_2(x, y) = \sum_{n=0}^{+\infty} (A^2_{2n+1} \sinh mx + B^2_{2n+1} \cosh mx) \sin my$$

$$m = \frac{(2n + 1)\pi}{2c}$$

It is immediately seen that the boundary conditions are as follows:

(i) $\dfrac{\partial \vartheta_1}{\partial x} = 2y \qquad (x = b)$

$$\frac{\partial \vartheta_1}{\partial y} = 0, \frac{\partial \vartheta_2}{\partial y} = 0 \quad (y = c, y = -c)$$

(ii) $\mu_1 \dfrac{\partial \vartheta_1}{\partial x} - \mu_2 \dfrac{\partial \vartheta_2}{\partial x} = 2y(\mu_1 - \mu_2)$

$(x = a, x = -a)$

(iii) $\vartheta_1 = \vartheta_2 \qquad (x = a)$

In order to satisfy these boundary conditions, it will be remembered that in the interval $(-c, +c)$ the function $2y$ may be expressed as a series expansion:

$$2y = \sum_{n=0}^{+\infty} mA_{2n+1} \sin my$$

where:

$$m = \frac{(2n + 1)\pi}{2c}$$

$$A_{2n+1} = 4c^2 \left(\frac{2}{\pi}\right)^3 \frac{(-1)^n}{(2n + 1)^3}$$

This series is a Fourier series for the function f defined as follows in the interval $(-2c, +2c)$:

$f = 2y$ in the interval $(-c, +c)$

$f = 4c - 2y$ in the interval $(c, 2c)$

$f = -4c + 2y$ in the interval $(-c, -2c)$

The boundary conditions may be written as follows:

(i) $A^2_{2n+1} \cosh mb + B^2_{2n+1} \sinh mb = A_{2n+1}$

(ii) $\mu_1 A^1_{2n+1} \cosh ma - \mu_2 A^2_{2n+1} \cosh ma$
$- \mu_2 B^2_{2n+1} \sinh ma = A_{2n+1}(\mu_1 - \mu_2)$

(iii) $A^1_{2n+1} \sinh ma - A^2_{2n+1} \sinh ma$
$- B^2_{2n+1} \cosh ma = 0$

Solving the three preceding equations with respect to the quantities A^1_{2n+1}, A^2_{2n+1} and B^2_{2n+1} one obtains the torsion function φ, i.e. the solution of the torsion problem:

$$\varphi_1(x, y) = \vartheta_1(x, y) - xy$$

$$\varphi_2(x, y) = \vartheta_2(x, y) - xy$$

where:

$$\vartheta_1(x, y) = \sum_{n=0}^{+\infty} A^1_{2n+1} \sinh mx \sin my$$

$$\vartheta_2(x, y) = \sum_{n=0}^{+\infty} (A^2_{2n+1} \sinh mx + B^2_{2n+1} \cosh mx) \sin my$$

$$m = \frac{(2n + 1)\pi}{2c}$$

$$A^1_{2n+1} = [\mu_2 + (\mu_2 - \mu_1)(\sinh ma \sinh mb - \cosh ma \cosh mb)]\Delta$$

$$A^2_{2n+1} = [\mu_1 \cosh^2 ma - \mu_2 \sinh^2 ma$$

$$+ (\mu_2 - \mu_1)\sinh ma \sinh mb]\Delta$$

$$B^2_{2n+1} = [(\mu_1 - \mu_2)\sinh ma(\cosh mb - \cosh ma)]\Delta$$

with:

$$\Delta = A_{2n+1}[\cosh ma \sinh ma \sinh mb(\mu_2 - \mu_1) + \cosh mb(\mu_1 \cosh^2 ma - \mu_2 \sinh^2 ma)]^{-1}$$

$$m = \frac{(2n+1)\pi}{2c}$$

The torsion moment M in this case has the form:

$$\frac{M}{\gamma} = 2\int_{S_1} \mu_1 \left(x^2 + y^2 + x\frac{\partial \varphi_1}{\partial y} - y\frac{\partial \varphi_1}{\partial x}\right) dx\,dy + 2\int_{S_2} \mu_2 \left(x^2 + y^2 + x\frac{\partial \varphi_2}{\partial y} - y\frac{\partial \varphi_2}{\partial x}\right) dx\,dy$$

that yields the torsional stiffness expressed as a series:

$$\frac{M}{\gamma} = \frac{8}{3}c^3[a\mu_1 + \mu_2(b-a)] + \sum_{n=0}^{+\infty} \frac{4}{m}(-1)^n A^1_{2n+1}\left(a\cosh ma - \frac{2}{m}\sinh ma\right)\mu_1 + \sum_{n=0}^{+\infty} \frac{4}{m}(-1)^n A^2_{2n+1}[(b\cosh mb - a\cosh ma) - \frac{2}{m}(\sinh mb - \sinh ma)]\mu_2$$

$$+ \sum_{n=0}^{+\infty} \frac{4}{m}(-1)^n B^2_{2n+1}[(b\sinh mb - a\sinh ma) - \frac{2}{m}(\cosh mb - \cosh ma)]\mu_2$$

The solution of the torsion problem of isotropic rectangular bar [7], could be obtained taking $a = b$ or $\mu_1 = \mu_2$, in the preceding equations.

The numerical calculation of the complex torsional stiffness can be carried out introducing the complex shear moduli μ_1^* and μ_2^* separately measured by mechanical spectroscopy.

References

1. N. I. MUSKHELISHVILI, "Some Basic Problems of the Mathematical Theory of Elasticity" (P. Noordhoff Ltd., Groningen, Netherlands, 1963).
2. Z. HASHIN, *J. Appl. Mech.* **50** (1983) 481.
3. S. ETIENNE, in "Mechanical Spectroscopy in Material Science", edited by Magalas (Elsevier, Amsterdam, 1994), in press.
4. S. ETIENNE, J. Y. CAVAILLE, J. PEREZ, R. POINT and M. SALVIA, *Rev. Sci. Instrum.* **53** (1982) 1261.
5. H. BOURAHLA, J. CHAUCHARD, J. LENOIR and M. ROMAND, *Die Angewandte Macromolekular chemie* **178** (1990) 47.
6. E. DENGA and O. GZOWSKI, *Mater. Chem. Phys.* **19** (1988) 475.
7. S. TIMOSHENKO and J. N. GOODIER, "Résistance des Matériaux" (Librairie Polytechnique Béranger, Paris, 1961).

Received 27 May 1994
and accepted 9 November 1995